remote sensing

MDPI

Article

Monitoring Spatial-Temporal Variations of Lake Level in Western China Using ICESat-1 and CryoSat-2 Satellite Altimetry

Jun Chen [1,2] and Zheng Duan [3,*]

[1] School of Environment and Energy Engineering, Anhui Jianzhu University, Hefei 230601, China
[2] Anhui Engineering and Technology Research Center for Smart City, Anhui Jianzhu University, Hefei 230601, China
[3] Department of Physical Geography and Ecosystem Science, Lund University, 223 62 Lund, Sweden
* Correspondence: zheng.duan@nateko.lu.se

Abstract: The lakes in the arid or semi-arid regions of western China are more sensitive to climate changes, and lake levels are considered as a direct indicator of regional climate variability. In this study, we combined satellite altimetry data from ICESat-1 with a smaller footprint and higher accuracy (compared to radar altimetry) and CryoSat-2 with a higher resolution in the along-track direction to monitor lake levels in western China and their trends over a long time period from 2003 to 2021. Our satellite altimetry derived lake levels were well-validated by comparing them against in situ measurements for a lake and independent altimetry-derived product from the DAHITI database for the common lakes. Furthermore, the commonly used linear model was applied to our derived lake level time-series to estimate the overall change trends in 67 typical lake levels over western China. Our results showed that 55 (82%) of these lakes displayed an increasing tendency in water levels, and the remaining 12 (18%) lakes showed a decreasing trend. Overall, the mean water level changing rate in western China was +0.15 m/yr (−1.40 to +0.58 m/yr) during the studied time period. The spatial patterns of the lake level variations can be grouped into three subregions: lake level changes between 2003 and 2021 showed general rising lake levels for the central–northern TP (Tibetan Plateau) endorheic region and Xinjiang, but declining levels for the southern TP exorheic region. The seasonal characteristic of lake level changes showed a significant increase during the summer monsoon season, followed by decreases during the non-monsoon season. The precipitation variations play a leading role in the lake level changes in the context of warm and humid climate states. There were good correspondences between the monthly variations in the lake level and monthly mean precipitation. Additionally, the lake levels also showed a relationship with the air temperature change, in particular, the lake level increase showed a small degree of hysteresis behavior compared with the rising temperatures. Geographically, the precipitation increase in the westerlies regions led to widespread lake expansion in the central–northern TP and Xinjiang. Conversely, precipitation decrease in the Indian monsoon regions caused lake shrinkage in the exorheic region of the southern TP. This study helps us achieve a better understanding of the spatial-temporal patterns of lake level changes in the arid or semi-arid region of western China.

Keywords: water level; western China; radar altimeter; laser altimeter; lake

Citation: Chen, J.; Duan, Z. Monitoring Spatial-Temporal Variations of Lake Level in Western China Using ICESat-1 and CryoSat-2 Satellite Altimetry. *Remote Sens.* **2022**, *14*, 5709. https://doi.org/10.3390/rs14225709

Academic Editors: Tomislav Bašić, Marijan Grgić and Giovanni Battista Chirico

Received: 13 September 2022
Accepted: 9 November 2022
Published: 11 November 2022

1. Introduction

The total area of lakes with a surface area larger than 1.0 km^2 in China is about 8104 km^2 [1], and half of the total area is contributed by lakes in western China. Moreover, 14 of China's 28 largest lakes (areas > 500 km^2) are saline [2], and all of these large salt lakes are located in the Tibetan Plateau (TP) and Xinjiang. So far, only a few studies have investigated the climatic effects on the lakes in arid or semi-arid regions of western China [3], mainly due to the limited availability of in situ measurements because of the harsh natural environments and relative inaccessibility [4]. However, hydrological regimes

in arid or semi-arid zones are more vulnerable to climate change than hydrological regimes in humid regions [5], calling for more studies on these arid or semi-arid areas. In recent decades, the physical properties of western China's lakes have been strongly affected by regional climate changes and human activities. For example, the shrinkage and vanishing of several lakes in Xinjiang occurred because of climate warming [6] and increased agriculture irrigation [7]. In contrast, the expansions of alpine lakes on the TP are considered to be tightly associated with glacier retreating and permafrost thawing [8] as well as changes in precipitation and evapotranspiration [9].

As an important indicator of lake changes, the lake mass balance can be estimated through water inputs (including river inflow, precipitation over the lake, and groundwater recharge, etc.) and outputs (including river outflow, evaporation from the lake, and groundwater seepage, etc.) [10]. Unfortunately, the direct measurement of these hydrological variables at gauging stations is usually limited due to many reasons such as financial issues. Moreover, the harsh natural environment and relative inaccessibility in western China present further challenges. In this context, satellite remote sensing technologies have proved to be powerful and efficient tools for monitoring lakes in western China [11]. Satellite altimetry has been an efficient technique and is widely used to monitor lake level variations [12], especially radar altimeters such as Topex/Poseidon, Jason, and ENVISAT, etc. can be used to measure lake levels and in combination, their data could cover 30 years since 1992 [13]. However, these radar altimeters are more suitable for large water bodies and many lakes are only visited by one or two satellites due to their large footprint and large track spacing. Conversely, laser altimetry with a smaller footprint and generally higher accuracy (compared to radar altimetry) is considered to be more suitable for monitoring the water level of small lakes; ICESat-1 altimetry data over the water surface in the TP and central Asia have been examined by numerous studies and have been shown to have a high precision [14–17]. However, the ICESat-1 only provides data over a short time period, 2003–2009 [18]. Fortunately, CryoSat-2 was launched in 2010, which can monitor lake levels for the period following the ICESat-1 data [19]. Furthermore, the CryoSat-2's density of ground tracks is relatively high compared to other radar altimeters, thereby making CryoSat-2 cover more small lakes [20].

There are a few studies that have used ICESat-1 or CryoSat-2 data to obtain the lake levels. However, previous studies have either mainly used the single altimetry data to monitor a large number of lakes [17,19,20], or focused on only the individual large lakes by combining data from multiple satellite altimetry [21,22]. In this work, we aimed at combining satellite altimetry data from ICESat-1 and CryoSat-2 to monitor the lake level variation of a large number of lakes (67 lakes) and their trends in a complete and long time period (2003–2021), covering the whole arid or semi-arid region of western China. So far, how to disentangle the contributions of precipitation and glacier melt to lake mass balance are still open questions, mainly due to the lack of continuous in situ observations of the monthly or seasonal lake level variations. To overcome the above-mentioned challenges, data from CryoSat-2 with a short repeat subcycle and high precision can be used to investigate the monthly and seasonal lake level variations in the whole of western China, which has not previously been possible. Specifically, the objectives of this study were to: (1) analyze the overall temporal trends and spatial patterns of 67 large lake level changes from 2003 to 2021; (2) investigate the monthly and seasonal variations in lake levels and take four typical lakes on the Qiangtang Plateau as examples to link the lake level seasonal cycles with regional climate variations (e.g., precipitation and air temperature); and (3) evaluate the spatial heterogeneity for the climate driving mechanism of lake level change, under the context of warm and humid climate states. This work is expected to help us achieve a better understanding of the spatial-temporal variation patterns of lake levels in the arid or semi-arid region of western China.

2. Study Area

Three provinces (including Tibet, Xinjiang, and Qinghai) located in the arid/semi-arid region of western China were defined as the study area, which has an area of more than 4 million km^2, accounting for a large percentage of areas of China. Therefore, any long-term lake changes could affect the water resource balance and the hydrologic cycle of the whole of China. The lakes in the arid and semi-arid regions of western China are generally adjacent to oases, and these inland lakes are the major growing regions of fishing in western China. Additionally, these lakes will play an important role in tourism development and transportation construction under the context of "the Belt and Road". There are more than 1500 lakes in western China [23]. In this work, our initial analysis with a large number of experiments showed that the uncertainties of water level monitoring were too large and unacceptable when the water extent size was below 150 km^2. Therefore, the 67 largest lakes with an area of larger than 150 km^2 were selected as the studied lakes. As shown in Figure 1, there are 63 alpine lakes distributed on the TP (Tibet and Qinghai), and the other four inland lakes are distributed in Xinjiang. All of these typical lakes are mainly distributed over the 11 basins including the Qiangtang endorheic region, Yangtze Basin, Yellow Basin, Brahmaputra Basin, etc. In contrast to the freshwater lakes in eastern China, glacier meltwater is a crucial supply source for the lakes in western China.

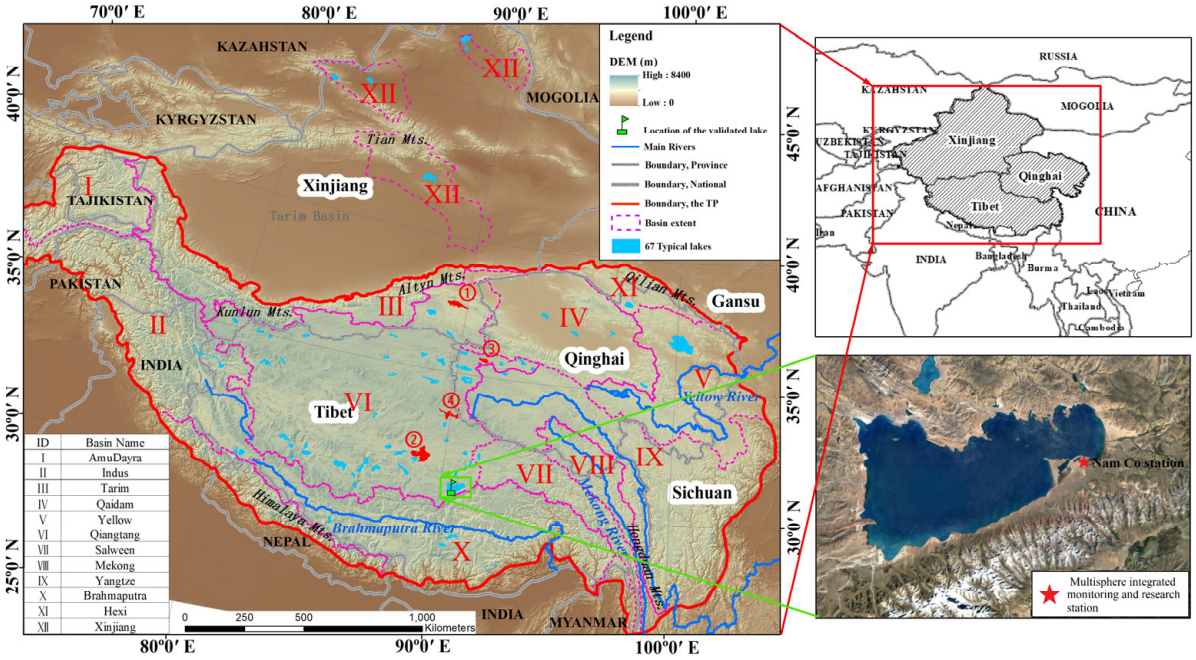

Figure 1. Topographic map of western China and the distribution of 67 of the studied lakes (are shown in blue) and main rivers. The grey shaded area in the top-right inset indicates the study area. ①, ②, ③, and ④ indicate Ayakkum, Se-lin Co, Hoh Xil, and Dorso Cave Co, respectively. The green flag indicates the validated lake with the in situ water level observations (Nam Co). The purple dotted lines indicate the extent of the twelve main basins.

3. Data and Methodology

Figure 2 shows the flowchart of the data processing and methods used for deriving the lake level changes from ICESat-1 and CryoSat-2 altimetry data and analysis in this study. The subsections describe the data and key processing and analysis methods in more detail.

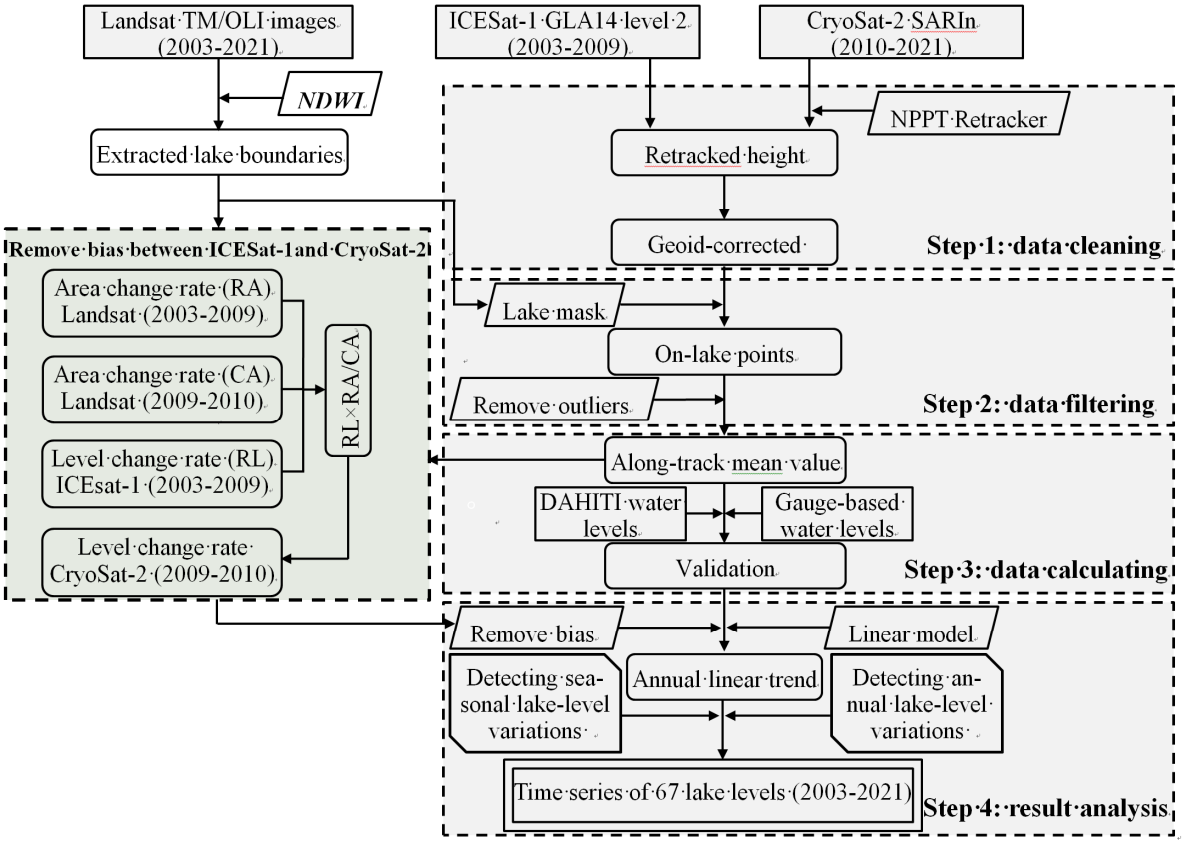

Figure 2. The flowchart of the data processing and methods used for deriving the lake level changes from the ICESat-1 and CryoSat-2 altimetry data in this study. The data processing includes four main steps as follows. Step 1. Data cleaning: Water elevations must be geoid corrected and retracked; Step 2. Data filtering: The footprints that fall entirely within the lake boundaries were selected and outliers were removed. Additionally, the bias between the two differential altimetry measurements must be removed; Step 3. Data calculation: The lake levels were estimated by averaging the water elevations of the remaining valid observations. Meanwhile, it is also necessary to demonstrate the validation of two altimetry data in detail; Step 4. Result analysis: A linear model was applied to our derived lake level time-series to estimate the overall change trends in 67 typical lake levels.

3.1. Landsat Images and Processing

The lake boundaries during 2003–2021 were extracted from more than 200 Landsat Thematic Map (TM) and Operational Land Imagery (OLI) images using the normalized difference water index (*NDWI*) method (Equation (1)) [24].

$$R_{NDWI} = \frac{r_{green} - r_{nir}}{r_{green} + r_{nir}} \quad (1)$$

r_{nir} and r_{green} indicate the near-infrared band and the green band, respectively. The *NDWI* values ranged from −1 to 1, and we applied the classification threshold that was advocated by Kumari et al. (2021) to extract the water extent [25].

3.2. CryoSat-2 Radar Altimetry Data and Processing

The CryoSat-2 satellite was launched on 8 April 2010, with the primary goal of monitoring the variations in ice sheets and sea ice. CryoSat-2 satellite has a 369 days repeat cycle and a 30-day subcycle [26]. The spatial coverage of the CryoSat-2 ground tracks is very high (7–8 km spacing at the equator). The denser spatial sampling means that smaller glaciers and water bodies can be monitored more frequently. A new radar altimeter (Synthetic Aperture Radar Interferometric Radar Altimeter, SIRAL) was carried

on CryoSat-2, which operates in three different modes: Low-Resolution mode, SARIn mode (Ku-band) mode, and SAR mode [27]. In this work, Level-2 SARIn mode altimetry data were employed, covering the period from July 2010 to April 2021; the best accuracy was about 30 cm for the SARIn mode [27]. The data were downloaded at https://earth.esa.int/eogateway/missions/cryosat/data (accessed on 10 July 2022). Figure 3 shows the ground tracks of CryoSat-2 used in this study, and four example lakes (Ayakkum, Se-lin Co, Hoh Xil, and Dorso Cave Co) are presented for illustrative purposes.

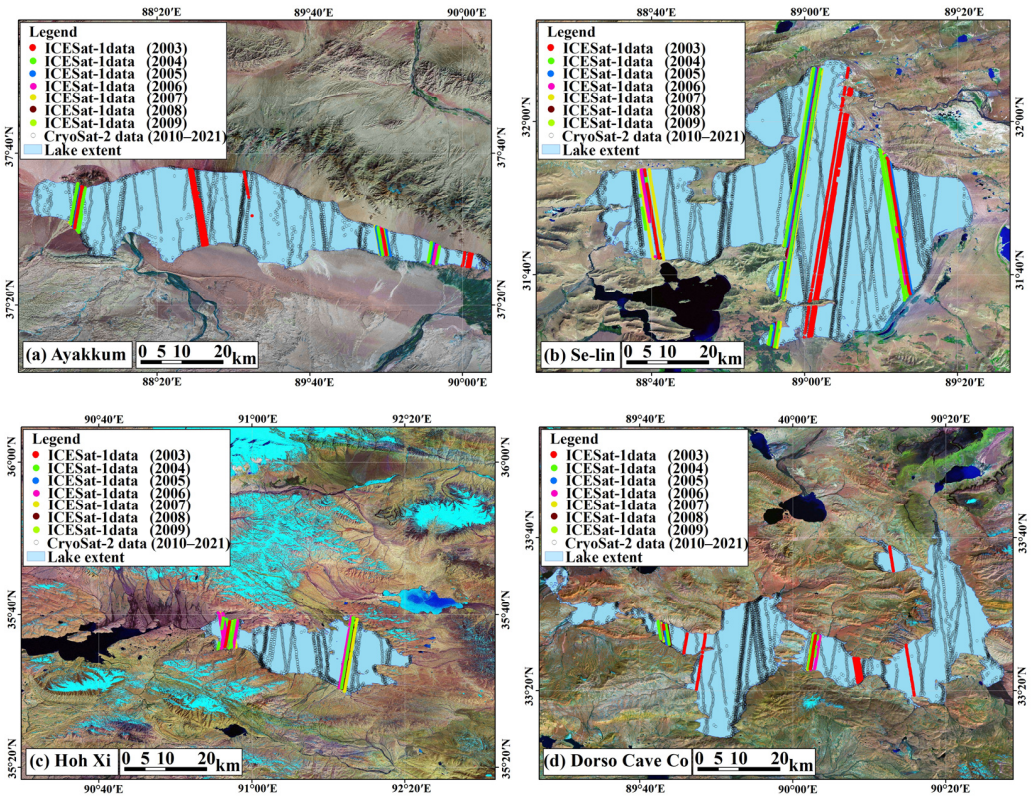

Figure 3. CryoSat-2 and ICESat-1 tracks (valid footprints) through Ayakkum (**a**), Se-lin Co (**b**), Hoh Xil (**c**), and Dorso Cave Co (**d**). Different color points indicate ICESat-1 tracks in different years, and all CryoSat-2 tracks are given in grey because of the high density of the CryoSat-2 data.

We extracted the lake levels using the four main steps as follows: Step 1. Data cleaning: Daily water elevations were extracted from the CryoSat-2 Level-2 geophysical data record (GDR) datasets using MATLAB software; then the narrow primary peak threshold (NPPT) retracker was employed to improve the valid results for water applications, which had been introduced in detail by Jain et al. (2015) [28,29]. The lake surface altitude of each footprint was corrected using an empirical formula that had been demonstrated in detail by Chen et al. (2020) [30]. Step 2. Data filtering: Selecting footprints that fall entirely within the lake boundary, and removing outliers outside of one standard deviation. Step 3. Data calculation: The lake levels were estimated by averaging the water elevations of the remaining valid observations. Meanwhile, the accuracy of the water levels derived from CryoSat-2 were validated by comparing against in situ measurements for a lake and the independent altimetry-derived product from the DAHITI database for the common lakes. Step 4. Result analysis: A linear model was applied to our derived lake level time-series to estimate the overall change trends in 67 typical lake levels.

It should be noticed that the CryoSat-2 altimetry data are referenced to the World Geodetic System 1984 (WGS84) and Earth Gravity Model (EGM) 96. However, in situ measurements of the lake water level data at gauging stations in China are generally referenced to the 1985 National Vertical Datum [22]. In order to make a fair comparison for evaluation purposes, the elevation values from the WGS84 EGM96 Geoid were transformed

using a constant height offset of 0.4 m, which represents the difference between the ellipsoids of the WGS84 EGM96 and 1985 National Vertical Datum following previous studies [31,32].

3.3. ICESat-1 GLA14 Product and Processing

The ICESat-1 satellite was launched on 3 January 2003 and ended in February 2010. The ICESat-1 carries the Geoscience Laser Altimeter System (GLAS), which can provide global observations of ice, aerosol and cloud heights, land topography, and vegetation characteristics with high precision [33]. ICESat/GLAS has small footprints and along-track observation distances, which is superior to radar altimeters in data availability and accuracy. Therefore, ICESat altimetry has been widely employed to monitor water levels [16,17] and has shown a relative accuracy of better than 10 cm [32]. The ICESat-1 GLA14 level 2 Global Land Surface Altimetry product (February 2003 to October 2009) provides global land surface elevations (including reservoirs, lakes, and rivers), geodetic, range measurements, plus footprint centroid geolocation, atmospheric, and instrumental corrections, and many other parameters [34]. All GLA14 Release-33 laser altimetry data can be downloaded from the U.S. National Snow and Ice Data Center (NSID) at https://nsidc.org/data/ (accessed on 20 February 2022). The ICESat-1 elevations are referenced to the Topex/Poseidon ellipsoid and EGM 96 Geoid. Thus, we first converted them to the WGS84 ellipsoid elevations using Equation (2), which has been demonstrated in detail by Zhang et al. (2011) [17]:

$$\text{Water } levels_{WGS84} = ICESat_{levels\ measured} - ICESat_{geoid} - 0.7 \quad (2)$$

where the $ICESat_{levels\ measured}$ and $ICESat_{geoid}$ are directly provided by the NSID referenced to Topex/Poseidon ellipsoid, and the constant of 0.7 m indicates a constant height offset between the Topex/Poseidon ellipsoid and WGS84 ellipsoid [32].

We also converted the WGS84 EGM96 Geoid to the 1985 National Vertical Datum with an offset of 0.4 m [31]. The main procedures for deriving lake levels from ICESat-1 data are the same as the CryoSat-2 data described in Section 3.2. Note that the NPPT tracker was only used for retracking the processing of radar altimetry data, not for ICESat-1. For illustrative purposes, Figure 4 shows the identification of outliers using one standard deviation and lake boundary for extracting the valid observations for water level estimation in Hoh Xil.

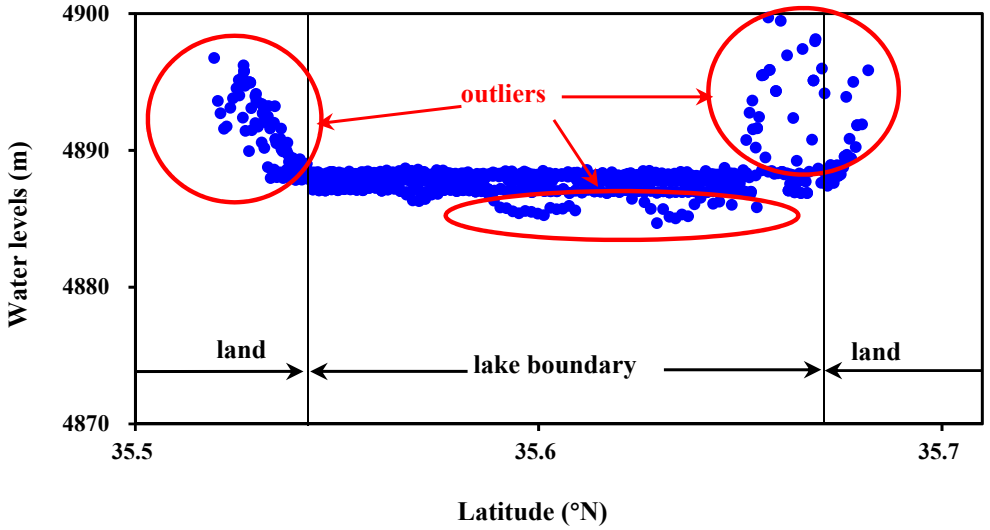

Figure 4. The elevation profiles of ICESat-1 GLA14 tracks through the eastern Hoh Xil from 2003 to 2009. Note that the wavelet-noise is generally the result of a series of natural disturbances; as a result, ICESat-1 data still have a few outliers in the middle of the lake as well as a few outliers in the land area on both sides of the lake.

3.4. Meteorological Data and Processing

Temperature and precipitation grid data on the TP from 1998 to 2017 were provided by the National Tibetan Plateau/Third Pole Environment Data Center (TPDC). Metadata are gathered from the daily air temperature and precipitation data from high-density ground stations in China [35]. In this work, we extracted annual and monthly variations in mean precipitation and air temperature of two subregions on the TP from 2003 to 2017, using the method of overlaying the TPDC grid data and the boundaries of subregions. Additionally, the annual mean precipitation and air temperature from 2003 to 2017 of the Xinjiang region were obtained from the Xinjiang Meteorological Center.

3.5. In Situ Lake Levels and DAHITI Database

Gauge-based water level data for the large lake Nam Co were used to evaluate the derived lake levels using CryoSat-2 or ICESat-1 altimetry data in the previous studies [17,36]. The gauge-based daily water levels of Lake Nam Co have been made available by the Chinese Academy of Sciences from 2005 with quality control. Daily measured lake levels of Nam Co for the time period 2007 to 2016 were obtained from TPDC [37] and used to evaluate our derived lake level (Figure 1). The validation methods by Siddique Akbor et al. (2011) were used to evaluate the accuracy of our derived lake levels [38]. As stated in previous sections, we converted the satellite altimetry derived water elevations to a target datum (1985 National Vertical Datum) for inter-comparison. The correlation coefficient (R) was used to evaluate the agreement between satellite altimetry elevations and in situ observations following previous studies [10,36].

As mentioned in Section 1, the measured lake levels are very limited in the study area. Fortunately, other independent satellite altimetry derived products of lake levels can be used for comparison in order to obtain hints into the quality of our derived lake levels in this study. One of the most comprehensive satellite altimetry derived products is the Database for Hydrological Time Series of Inland Waters (DAHITI) [39]. The DAHITI was developed by the Technical University of Munich, and it now provides more than six hundred water elevation time-series of rivers, reservoirs, and lakes using multi-sources and multi-sensor satellite altimetry data. The DAHITI only provides lake levels for 41 lakes across the whole of China, and most lakes in the Tibet Plateau and Xinjiang are not included, which motivated us to derive the lake levels in more lakes by directly processing the satellite altimetry data in this study. The lake levels from DAHITI have been well-validated in many lakes and showed a good accuracy of better than 30 cm [40,41]. However, it should be noted that DAHITI data are derived from multi-source and multi-sensor satellite altimetry data, and thus there can be differences in many aspects (data sources, underlying methods, actual dates of the lake levels, reference datum etc.) between the DAHITI data and our derived lake levels. Therefore, we did not directly compare the absolute values in lake levels from our derived ones and DAHITI due to the aforementioned possible differences. Instead we applied the same linear model to both the DAHITI lake levels and our derived lake levels, then we compared the detected trends to illustrate the consistency between them. In short, we believe that the accuracy of our derived water levels can be well-validated by a comparison with the DAHITI data. The DAHITI lake levels for the two common lakes Se-Lin and Ayakkum were downloaded from https://dahiti.dgfi.tum.de/en/products/water-level-altimetry/ (accessed on 18 July 2022).

3.6. Removing Systematic Elevation Bias and Estimating Linear Change Trends

There is still a need to remove systematic elevation bias due to the influencing factors such as altitude, equipment, orbit, and inclination used by each satellite even though the ICESat-1 and CryoSat-2 data have been referenced to the same ellipsoid (WGS84). Currently, the method most commonly used to remove this systematic bias between different satellite data is to make comparisons of the mean water level difference over an overlapping period [42]. Unfortunately, there was no overlap period between CryoSat-2 and ICESat-1 data. To assess the basis between two altimetry data, the lake level change (2009–2010)

can be calculated by an equation of RL × RA/CA. RA indicates the lake area change rate (2003–2009), CA indicates lake area change rate (2009–2010), and RL indicates lake level change rate (2003–2009). Xu et al. (2022) demonstrated the reasonable performance of this method and reported that any errors were manageable revealed by the estimated lake level values despite the uncertainties inherent in this approach [43].

Finally, we used a linear model (Equation (3)) to estimate the overall change trends in lake levels [44]. The changing trend was estimated by fitting the following equation to the observations using a least squares method:

$$y = \beta_0 + \beta_1 t \quad (3)$$

where y indicates the lake level time series; β_0 and β_1 indicate the parameters to be estimated; and t is the time (decimal year). β_1 indicates the line trend (m/yr).

4. Results

4.1. Validation with In Situ Lake Levels and Comparison with DAHITI Database

Figure 5 shows the comparison of in situ lake levels and derived lake levels from satellite altimetry. The CryoSat-2 and ICESat-1 altimetry lake levels were highly correlated with the gauge-based water levels from Nam Co station, with a relatively high correlation coefficient of 0.79 (2010–2016) and 0.93 (2007–2009) for Nam Co, respectively. Our results are consistent with the report by Song et al. (2015) of 0.712 (2010–2013) and 0.98 (2006–2009) [36]. The validation results indicate very good consistency between the CryoSat-2 and ICESat altimetry derived lake levels, and the in situ measurements.

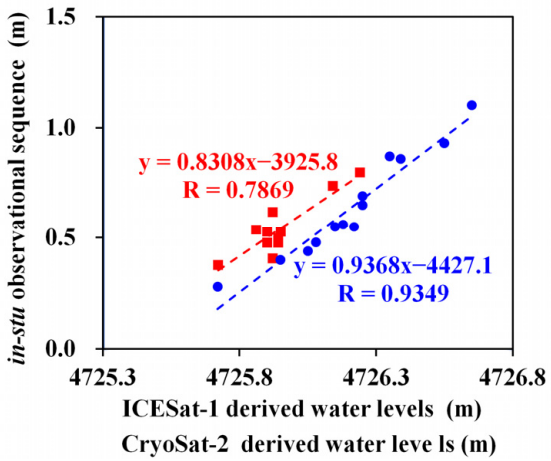

Figure 5. The correlation between the ICESat-1 (shown in blue) and CryoSat-2 (shown in red) altimetry derived lake levels and the in situ measured lake levels. It can be noted that the gauge-based water level data took the observational data (beginning with 0.0 m) at the beginning of every year as a reference, and an observational sequence was generated every year.

Figure 6 shows the comparison of the estimated trends in the lake level changes in two common lakes, Se-Lin and Ayakkum, using our derived lake levels and the DAHITI product. A relatively large height offset between DAHITI and ICESat-1 was observed for Lake Se-Lin, which could be caused by the possible differences (mentioned earlier in Section 3.5), with the main reason being the difference in the reference datum used between DAHITI and our derived data. As mentioned earlier, we only focused on comparing the calculated trends. The results clearly showed that the monthly rates of change using our derived lake levels are in good agreement with those from the DAHITI product, with a small difference in the estimated trends within 0.02 m/yr. This good agreement proves the good quality of our derived lake levels and gives us confidence in using our derived lake levels for monitoring the lake dynamics and estimating the trends.

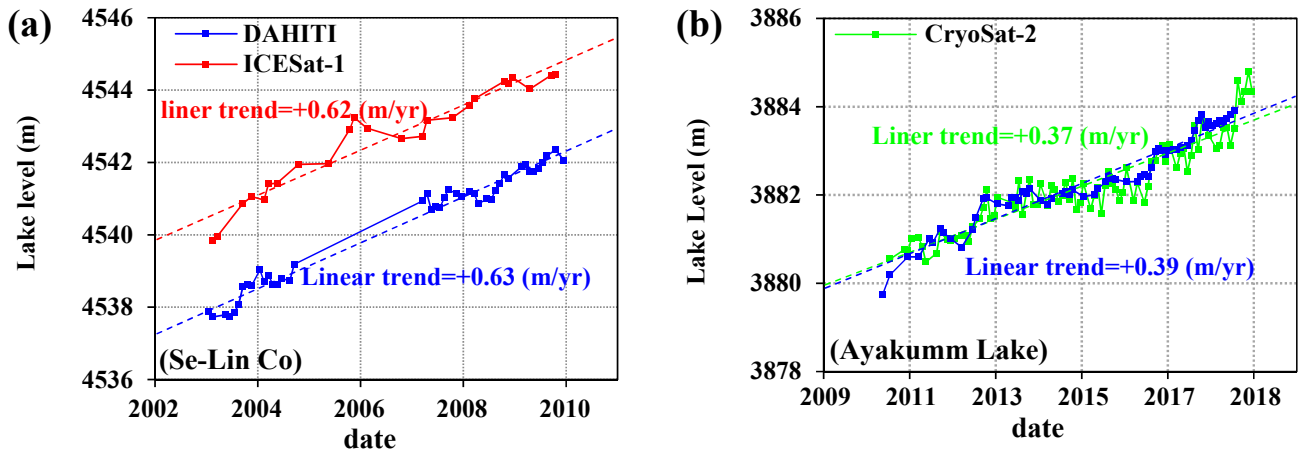

Figure 6. Comparison of the estimated trends using the DAHITI product and our derived lake levels from (**a**): ICESat-1 for Lake Se-Lin Co and (**b**) CryoSat-2 for Ayakkum.

4.2. The Detailed Characteristics of Water Levels Changes in Four Typical Lakes

There are 28 lakes that exceed 400 km^2 over the study area. We excluded large lakes with high social attention such as Qinghai and Nam, etc., because these lakes had been widely monitored in previous studies. Moreover, in order to correspond to the contents of climate drivers of lake change over inner TP in the later Discussion section, four closed lakes (i.e., Ayakkum, Dorso Cave Co, Hoh Xil and Se-lin) across the Qiangtang Plateau were selected to investigate the water level seasonality and annual trends in more details.

4.2.1. Interannual Variations in Water Level for Four Typical Lakes

As shown in Figure 7, all four lakes showed continuous and clear increasing trends during the observation period. The water level of Ayakkum increased from 3879.3 m in February 2003 to 3884.9 m in March 2021, increasing by 5.6 m in total, at a rate of 0.27 m/yr from 2003 to 2021. Se-lin was previously claimed as having the fastest water level increase in the TP [45], which had one of the largest increase rates (+0.51 m/yr) in the 67 studied lakes, and it showed a dramatic increasing trend at a rate of 0.77 m/yr during the early observation period (2003–2011). The water level of Se-lin Co increased 9.19 m, from 4540.0 m in March 2003 to 4549.2 m in March 2021. Hoh Xil and Dorso Cave Co also showed strong increasing trends over the observation period with an annual changing rate of 0.41 m/yr and 0.42 m/yr, respectively.

4.2.2. Monthly and Seasonal Characteristics of Lake Level Variations

Compared with the ICESat-1 data that cover only 4 months in a year, the high temporal coverage of CryoSat-2 data allowed for monthly and seasonal trends to be explored.

Figure 8 shows the monthly variations in the lake levels derived from CryoSat-2 in the four typical lakes during 2010–2021. It must be pointed out that the month of the highest lake levels was determined by the month when the maximum measured value of the water level occurs, and the beginning month of the lake level increase is determined by the phenomenon that the water level has continuously increased from a certain month. Significant lake level increases during the summer monsoon season (generally occur during June-October) were followed by decreases during the non-monsoon season. The increase in the four typical lake levels began in late May or early June with the highest levels reached in late September to middle October. After that, the lake levels decreased considerably until late December to early January of the next year when the lake surface froze. The ice coverage led to water levels tending to stable during the frozen period. After the melt of lake ice in March or April, the lake levels decreased until the onset of the summer monsoon. As shown in Figure 9, the mean change rate of four lake levels during 2003–2020 was similar

for each season, with values of +0.45 m/yr in spring, +0.35 m/yr in summer, +0.33 m/yr in autumn, and +0.48 m/yr in winter, and +0.41 m/yr for all seasons combined.

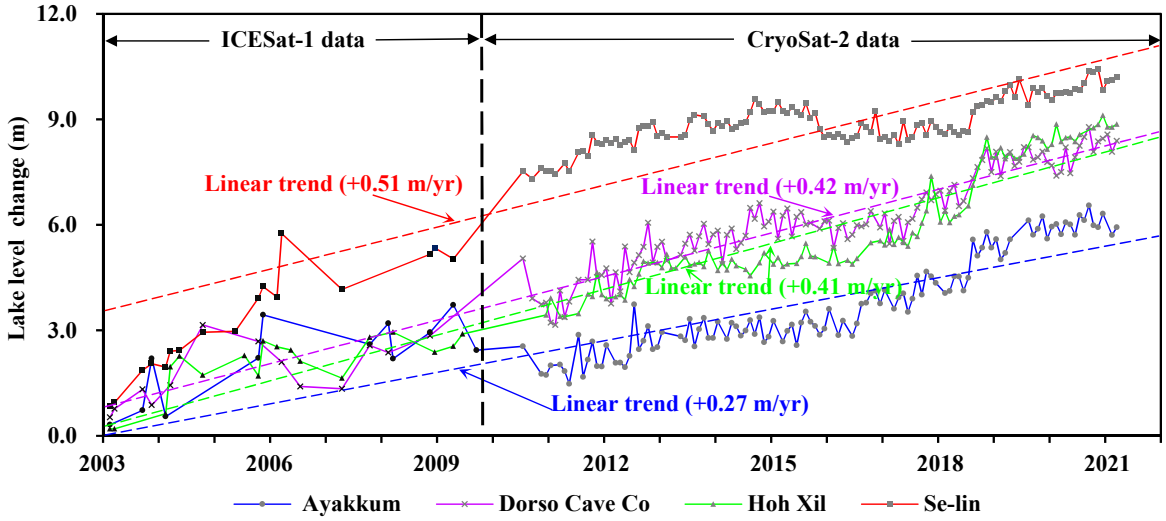

Figure 7. The estimated trends in our derived lake levels by combining the data from ICESat-1 (black dots) and CryoSat-2 (grey dots) for four typical lakes. Note that in order to gather the variation curves of the different lake levels, the water elevations were subtracted using a different constant for different lakes, respectively (e.g., Ayakkum (−3879), Dorso Cave Co (−4933), Hoh Xil (−4887), and Se-Lin (−4539)). Additionally, because ICESat-1 data only cover 4 months every year, the water level change curves of the four lakes did fluctuate markedly from 2003 to 2009 compared to the later water level changes derived from CryoSat-2 since 2010.

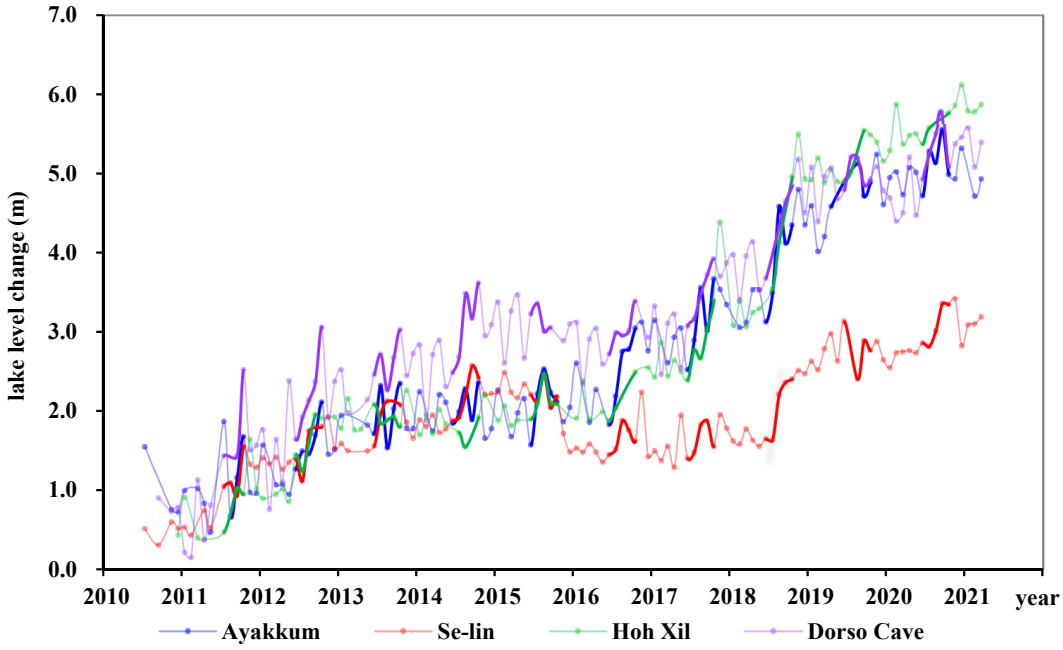

Figure 8. Monthly variations in the lake levels during 2010–2021, derived from the CryoSat-2 data. Note that the CryoSat-2 altimetry data only covered six months from July to December in 2010, and covered four months from January to April in 2021. The bold lines indicate the beginning and the highest month of lake level increase in different years (months 6 and 10).

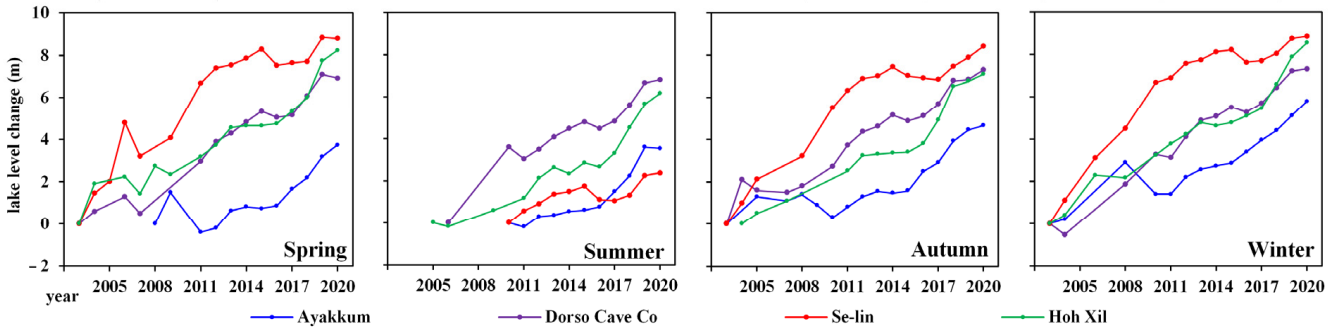

Figure 9. Lake level changes for four seasons during 2003–2021 derived from ICESat-1 and CryoSat-2. In order to gather the seasonal variation curves of lake levels of different lakes in the figures, the water level change curves were based on the monitoring start point.

4.3. Overall Water Level Changes of the 67 Studied Lakes

4.3.1. Temporal Variations of Lake Level in Western China

Table 1 presents a statistical summary of the lake levels and estimated trends in the lake level changes for all 67 studied lakes. A total of 51 lakes have relatively complete ICESat-1 elevation data covering the period of 2003 to 2009, and almost all of the studied lakes have complete CryoSat-2 data from 2010 to 2021. In total, 55 (82%) of these lakes showed an increasing tendency of water level, there were five lakes with an increasing rate rise by more than 0.5 m/yr, and Yang Hu had the most remarkable increase rate of 0.78 m/yr from 2003 to 2021. Two of the largest lakes are noteworthy; Se-lin showed a rapid increase trend at a rate of 0.51 m/yr from 2004 to 2021, and Se-lin has become the largest lake with an elevation of more than 4000 m on the TP. Qinghai Lake is the largest lake in China, whose water level increased by 4.13 m from 2004 to 2021 (at the rate of 0.23 m/yr). Conversely, the remaining 12 (18%) of the lakes showed a decreasing tendency, and Zonag had the largest decreasing rate (−1.4 m/yr). However, in large lakes with an area over 500 km^2, Yang-Cho-Yung showed the fastest decrease in water level, from 4441.9 m in March 2003 to 4437.9 m in March 2021, a 4.0 m drop during the 18 years (−0.46 m/yr). Overall, the mean elevation changing rate in western China was 0.15 m/yr (from −1.40 to +0.58 m/yr) for the 67 lakes with a clear increasing trend.

Generally, the amplitude of seasonal lake level variations in western China was considerably smaller than that of lakes in eastern China. There is a significant lake level increase during the summer monsoon season, followed by decreases during the non-monsoon season. The seasonal cycle of lakes in western China showed that the water levels rose continuously from May to August, and peaked between late August and early November, before falling rapidly from late October to early February in the next year.

Table 1. The lake water levels and statistics of the 67 studied lakes derived from the combined ICESat-1 and CryoSat-2 data. In the data coverage period from 2003 to 2021, a total of four monitoring periods were completed with about 5 years as a monitoring period.

Spatial Location	Lake Name	Start Date	Start Elevation (m)	Period 1 Date	Period 1 Elevation (m)	Period 2 Date	Period 2 Elevation (m)	Period 3 Date	Period 3 Elevation (m)	End Date	End Elevation (m)	Linear Trend
Brahmaputra	P'ei-k'u t'so	03/2003	4579.3	03/2006	4580	05/2011	4580.3	05/2015	4580.4	03/2021	4579.6	0.04
	P'u-mo-ts'o	02/2004	5011.1	03/2006	5011	11/2010	5012.2	11/2015	5012.1	09/2020	5012.4	0.14
Hexi	Yang-Cho-Yung	03/2003	4441.9	03/2006	4442.1	12/2010	4439.6	11/2015	4438.5	03/2021	4437.9	−0.46
	Har	05/2004	4077.8	03/2006	4077.8	10/2010	4078.4	11/2015	4079.3	03/2021	4081.5	0.21
Indus	Bangong	11/2003	4244.9	03/2006	4244.8	11/2010	4241.7	10/2015	4244.4	01/2021	4243.7	−0.07
	Langa					10/2010	4567.4	11/2015	4566.8	12/2020	4565.5	−0.11
	Mapam Yum	03/2003	4586.8	11/2005	4586.9	10/2010	4586.4	11/2015	4586.5	04/2021	4586.4	−0.03
Qaidam	Dabsan	02/2004	2677.8	10/2005	2678.3	10/2010	2679.5	11/2015	2678.6	04/2021	2679.8	0.1
	Donggi Cona	03/2003	4086.3			11/2010	4086.8	11/2015	4086.9	01/2021	4087.4	0.08
	Sitaginel	11/2003	2686.8	03/2006	2687.1	03/2011	2687.1	10/2015	2687.2	03/2021	2689.3	0.12
	Toson					09/2010	2805.8	11/2015	2810	02/2021	2813.6	0.76
Qiangtang	Aksayquin	02/2004	4852.5	03/2006	4852.8	11/2010	4849.8	11/2015	4850.9	03/2021	4852	0.07
	Ang-la jen	03/2003	4716.6	03/2006	4717.3	11/2010	4716.7	11/2015	4716.1	02/2021	4718.5	0.06
	Ang-tzu	03/2004	4687.4	05/2006	4688.2	11/2010	4689.6	10/2015	4690.6	02/2021	4691.6	0.26
	Aqqikkol	05/2004	4256.9	05/2006	4258.3	07/2010	4256.6	11/2015	4259.3	03/2021	4262.4	0.29
	Arkatag	03/2003	4720.9	11/2005	4723.1	11/2010	4716.8	10/2015	4718.8	02/2021	4722.6	−0.02
	Ayakkum	02/2003	3879.3	10/2005	3881.2	07/2010	3881.5	10/2015	3882.1	03/2021	3884.9	0.27
	Bangdag	03/2004	4910.2	03/2006	4910.9	04/2009	4913.7	11/2015	4913.8	10/2020	4917.8	0.44
	Zhari Nam	03/2003	4613.6	07/2005	4614.6	10/2010	4614.2	11/2015	4613.8	03/2021	4617	0.13
	Cha-pu-yeh ch'a-k'a					10/2010	4424.1	11/2015	4424.1	02/2021	4424.2	0.01
	Dagze	11/2003	4552.4	06/2006	4551.6	11/2010	4553.2	11/2015	4552.7	03/2021	4552.5	0.03
	Dogai Coring	02/2004	4819.2	02/2006	4820.3	11/2010	4820.8	11/2015	4821.3	03/2021	4822.8	0.19
	Dogen					12/2010	4554.2	12/2015	4554.1	12/2020	4553.6	−0.07
	Dorso Cave Co	03/2003	4933.8	03/2006	4935.1	11/2010	4936.7	11/2015	4938.9	03/2021	4941.4	0.42
	Duogecuoren					07/2010	4793.2	11/2015	4795.2	03/2021	4797.6	0.41
	Gozha						5080	11/2015	5079.7	12/2020	5080.1	0.03
	Hoh Sai	11/2003	4479.2	10/2007	4481.9	11/2010	4480	11/2015	4485.5	02/2021	4485.3	0.37
	Hoh Xil	10/2004	4888.7	05/2006	4889.4	12/2010	4890.4	10/2015	4892.1	03/2021	4895.9	0.41
	Hsu-ju					07/2010	4716.1	05/2015	4716.4	11/2020	4717.9	0.17
	Rinqin Xubco	02/2004	4761	10/2007	4761.7	01/2011	4761.9	04/2015	4762.6	12/2020	4764.1	0.17
	Jianshui hu	05/2004	4905.6	10/2007	4906.8	07/2010	4906.5	06/2015	4904.8	04/2021	4906.9	0.02
	Ko-jen	02/2004	4648	10/2007	4649	09/2009	4648.9	11/2015	4648.9	03/2021	4649.2	0.06
	Lixi'Oidain	11/2003	4872.3	10/2007	4873.3	07/2010	4874	05/2015	4876.1	03/2021	4879.8	0.7
	Lumajangdong	11/2003	4814.4	03/2006	4816.1	09/2011	4815.7	09/2015	4816.8	01/2021	4818.1	0.19
	Malgai tea card	09/2003	4798.4	03/2006	4803.1	11/2010	4799.4	05/2015	4801.2	01/2021	4804.1	0.22
	Memar	03/2004	4925.3	10/2006	4925.8	11/2010	4926.1	05/2015	4928.5	02/2021	4931.6	0.34

Table 1. *Cont.*

Spatial Location	Lake Name	Start Date	Start Elevation (m)	Period 1 Date	Period 1 Elevation (m)	Period 2 Date	Period 2 Elevation (m)	Period 3 Date	Period 3 Elevation (m)	End Date	End Elevation (m)	Linear Trend
	Mu-ts'o-ping-ni					12/2010	4687	12/2015	4686.5	12/2020	4686.7	−0.02
	Namru	11/2003	4568.4	11/2005	4571.6	11/2010	4571.4	11/2015	4572.7	02/2021	4572.8	0.23
	Na-Mu	03/2003	4723.2	03/2006	4724.9	11/2010	4726.2	11/2015	4726	03/2021	4726.1	0.16
	Ngoin	03/04	4564.5	03/2006	4563.2	11/2010	4565	11/2015	4564.4	03/2021	4565	0.05
	P'a-lung					03/2011	5101.1	03/2015	5101.8	03/2021	5102.6	0.15
	Pa-Mu-Ts'o					12/2010	4567.3	05/2015	4567.9	12/2020	4567.7	0.04
	P'eng-Ts'o					11/2010	4538.5	05/2015	4538.3	02/2021	4536.7	−0.1
	Qixiangcuo	11/2003	4615.1	03/2006	4617.5	03/2011	4619.5	07/2015	4620.5	02/2021	4620.7	0.33
	Rola Tso					07/2010	4818.3	11/2015	4820.1	03/2021	4822.5	0.25
	Salt Lake	03/2004	4462.7	03/2006	4465.3	03/2011	4450.7	11/2015	4458.5	02/2021	4466.9	0.04
	Se-lin	03/2003	4540	03/2006	4544.8	11/2010	4546.6	11/2015	4547.7	03/2021	4549.2	0.51
	T'a-jo	03/2004	4567.4	11/2005	4568.7	10/2010	4568.6	11/2015	4567.5	02/2021	4569.1	0.05
	Tang-je yung-ts'o	11/2003	4536.7	07/2006	4537.4	09/2010	4537.5	11/2015	4537.5	03/2021	4539.3	0.13
	Ta-tse	09/2003	4471.5	05/2006	4468	11/2010	4470.8	11/2015	4472.9	03/2021	4476	0.32
	Tupo	11/2003	4924.5	06/2006	4925.9	07/2010	4926.2	11/2015	4927	03/2021	4927	0.24
	Ulan Ula	11/2003	4857	03/2006	4859.7	07/2010	4859.3	05/2015	4861	02/2021	4862.7	0.47
	Vidration Spring	03/2003	4796.5	03/2006	4798.1	09/2010	4796.1	10/2015	4797.2	03/2021	4799.1	0.17
	Xijir Ulan	11/2003	4772.9	03/2006	4774.4	11/2010	4776.2	11/2015	4776.4	03/2021	4779.5	0.58
	Yaggain Canco	02/2004	4871.7	03/2006	4872.9	09/2010	4873.4	07/2015	4875.1	09/2020	4875.3	0.37
	Yang hu	11/2003	4787.6	03/2006	4789.7	10/2010	4789.2	11/2015	4791.7	02/2021	4796.4	0.78
	Yibug caka					02/2011	4556.7	11/2015	4556.8	12/2020	4558	0.12
	Zonag					12/2010	4756.2	10/2015	4743.6	03/2021	4742.4	−1.4
Salween	Na	11/2003	4586.8	03/2006	4585.1	12/2010	4585.1	10/2015	4586	01/2021	4586.8	0.04
	Ai-pi					10/2010	194.3	11/2015	194	03/2021	194.6	0.03
Xinjiang	Bosten	11/2003	1047.9	03/2006	1046.4	09/2009	1045.5	11/2015	1046.6	02/2021	1048.4	0.03
	Sai li-mu	02/2004	2074.1	10/2006	2074.6	10/2010	2074	11/2015	2074.2	02/2021	2074.7	0.03
	Ulungar	03/2003	483.4	05/2006	483.7	10/2010	484.4	07/2015	482	08/2020	483.6	−0.05
Yangtze	Dorge					12/2010	4686.8	11/2015	4686.9	03/2021	4686.5	−0.03
	Gyaring	02/2004	4292.1	10/2005	4293.2	10/2010	4293.7	11/2015	4293.4	03/2021	4292.8	0.04
Yellow	Ngoring					11/2010	4273.6	11/2015	4273.4	03/2021	4272.8	−0.05
	Qinghai	02/2004	3193.5	05/2006	3193.9	11/2010	3194.7	10/2015	3195.2	03/2021	3197.6	0.23

4.3.2. Spatial Patterns of Lake Level Variations

Figure 10 shows the spatial patterns of the lake level changes for all 67 studied lakes. Considering the different geographic and climatic features, 67 lakes can be grouped into three subregions: the central–northern TP endorheic region, the southern TP exorheic region, and Xinjiang. The overall spatial patterns of the lake level variations between 2003 and 2021 showed rising lake levels for the central–northern TP, but declining levels for the southern TP exorheic region.

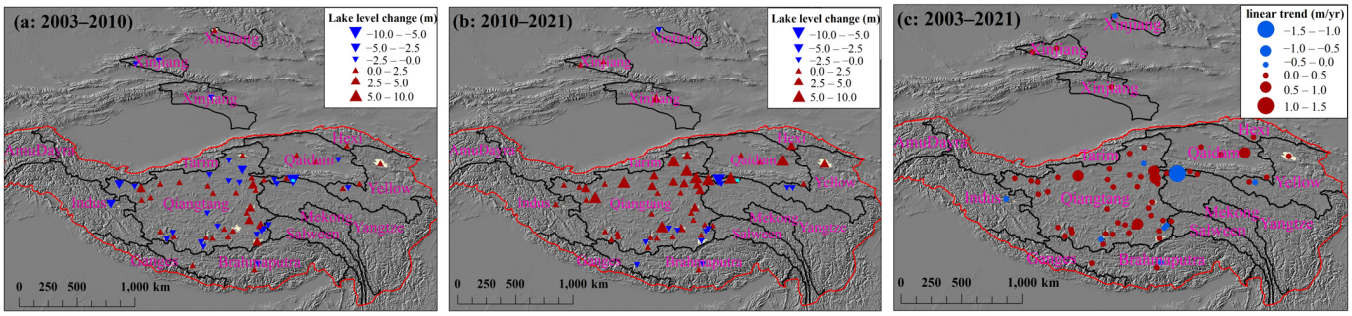

Figure 10. Spatial patterns of the lake level changes between 2003 and 2021. (**a**) and (**b**) show the lake level changes during 2003–2010 and 2010–2021, respectively. (**c**) shows the water level change rate (linear trend) during 2003–2021. The monitoring period of 16 relatively small lakes only covered 2010–2021 (as shown in Table 1), limited by the lack of reliable elevation data from ICESat-1.

(1) The central–northern TP endorheic region including the Qiangtang Plateau, Qaidam, Hexi, Yellow, Yangtze, and Salween River Basin. The Qiangtang Plateau is the most densely distributed area of lakes in China, and 47 lakes within this region were monitored. More specifically, the lakes with a water level increase are generally distributed in the central and northern Qiangtang Plateau. In particular, the alpine lakes in the Hoh Xil region showed a strong increase rate (e.g., 0.70 m/yr for Lixi'Oidain (2003–2021) and 0.58 m/yr for Xijir Ulan (2003–2021), etc.). The lakes with a water level decrease are generally distributed in the southern Qiangtang Plateau (e.g., −0.10 m/yr for P'eng-Ts'o (2010–2021) and −0.07 m/yr for Dogen (2010–2021), etc.). The seasonal trends in the majority of lakes across this subregion did slightly fluctuate from March to May, then smoothly increased from May to September, and reached their peaks between late September and early October. After that, the lake levels showed a continuous decrease from September to February of the next year. Qaidam and Hexi are located in the northeastern TP and include five lakes with a relatively small area. The mean changing rate showed an evident increasing tendency (0.25 m/yr), in particular, Toson showed the fastest increase in water level from 2010 to 2021 (0.76 /yr). The seasonal lake levels in this subregion rose continuously from May to June, then reached their peaks in August to November, while a few lakes did not do so until late November to December. The Yellow, Yangtze, and Salween River Basin, which is the origin of three large rivers including four small lakes, showed a slightly increasing tendency during the monitoring period. The seasonal cycle of lake levels in this subregion was similar to those of the lakes in Qaidam and Hexi.

(2) The southern TP exorheic region including Brahmaputra and the Indus River Basin. This subregion is located in the southern TP, and lakes are supplied from the glacier meltwater in the Himalayas. The mean changing rate showed a slight drop, which is consistent with the finding of Bian et al. (2009) that Yang-Cho-Yung had a negative balance in recent years due to the evaporation increasing under regional warming [46]. The seasonal characteristics of most lakes showed that the lake levels began to rise from March to May, but declined in June. They then rose from June to August and reached their peaks during August–September, then decreased with slight fluctuations until February.

(3) Xinjiang is located in arid central Asia, accounting for one-sixth of the total area in China. Therefore, lakes in Xinjiang play a critical role in the hydrologic cycle and water resource balance. There are five large lakes distributed in this region, four lakes with a

water level increase and only one lake with a slight decrease. It was noted that the largest inland freshwater lake (Boston) had a slightly increasing rate of 0.03 m/yr from 2003 to 2021. The change to seasonal characteristics of lake levels in Xinjiang were significant differences from the TP, seasonal changes showed a continuous increase since late March or early April, then reached peaks in late July or early August. After that, the lake levels decreased rapidly from September, and the decline reached its lowest point when the lakes began to freeze in January next year.

5. Discussion

5.1. The Lake Level Rise in the Context of a Warm and Humid Climate State

The change in lakes in the interior of western China is affected by precipitation, evaporation, and the glacier/permafrost melt water caused by a temperature increase. In this process, lake evaporation is closely related to water surface temperature and wind speed. However, compared with the dominant factors of lake change in Xinjiang that are easily determined, the main driving force behind dramatic lake dynamics over the TP has been under debate [47]. The existing studies have argued that temperature and precipitation playing leading roles in different periods, respectively. Specifically, from 1990 to 2000, the lake levels increased significantly because of the increased melting water due to the rising temperature. After 2000, precipitation became the main factor leading to the increase in lake water storage [48]. As shown in Figure 11, the precipitation in the central–northern TP and Xinjiang showed a clear increasing trend; our results also provide further evidence that most of western China has been in a warm and humid climate state since the beginning of the 21st century. Surprisingly, the annual mean precipitation in the southern TP exorheic region (e.g., Brahmaputra and Indus Basin) showed a slight decreasing trend. This is highly consistent with the spatial distribution characteristics of the lake level changes in western China (lake expansion in the northern TP and lake shrinkage in the southern TP were consistent with that of the precipitation increase in the westerlies and the decrease in Indian monsoon regions [49]).

5.2. Precipitation Seasonality and Lake Level Monthly Variations

In this work, we took the Qiangtang endorheic region and four typical lakes from there as an example to disentangle contributions of precipitation and air temperature to lake level variations based on CryoSat-2 data with short repeat subcycle and high precision. The overall feature is the good correspondence between the summer monsoon precipitation and lake level increases for four typical lakes. As shown in Figure 12, the larger amplitude of lake level increases generally occurred in relatively wet years (e.g., 2012, 2016, and 2017). Conversely, water levels of four typical lakes tend to be stable from 2013 to 2016, corresponding with relatively low precipitation in these dry years. The above corresponding relationship between precipitation and lake level variations provides further evidence that precipitation variations play a dominant role in the lake level changes in western China [50]. Additionally, the lake level monthly variations also showed a good relationship with the air temperature change; in particular, the lake level increase showed a small degree of hysteresis behavior compared with the rising temperatures. This hysteresis provides extra evidence that the meltwater increase caused by regional warming has an important impact on the lake level increase.

5.3. Spatial Heterogeneity for Climate Driving Mechanism of Lake Level Change

As mentioned in the Results section, the spatial patterns of the water level variations of 67 lakes can be grouped into three subregions (Figure 13). Subregion A is the central–northern TP endorheic region. The water level changes were affected by both the precipitation and glacial meltwater and showed a positive trend. Although the meltwater from glaciers, permafrost, and spring snow was a vital source of supplies [51–53], the summer precipitation rising in the westerlies region plays a leading role in lake expansion in this subregion [49]. Subregion B is the exorheic region of the southern TP, mainly affected

by the Indian monsoon, and the decrease in precipitation from the Indian monsoon over the past years has led the lake levels in the Brahmaputra and Indus River Basin to fluctuate more, and to decline continuously [54]. The increase in glacier meltwater did not lead the lake over the exorheic region of the southern TP to expand significantly in the context of warm-dry climate conditions [55]. Subregion C is mainly located in Xinjiang. Except that Sai li-mu is steadily supplied by glacier meltwater [14], the other three lakes are mainly supplied by runoff from precipitation. Among them, human activities such as irrigation, etc. have exerted a decisive influence on the Bosten water volume changes, suffering from dam construction at the lake outlet [56]. The precipitation increase in climate conditions of warm and humid had a primary impact on lake expansion in the arid region of Xijiang [57]. In short, precipitation plays a leading role in the lake level variations over western China.

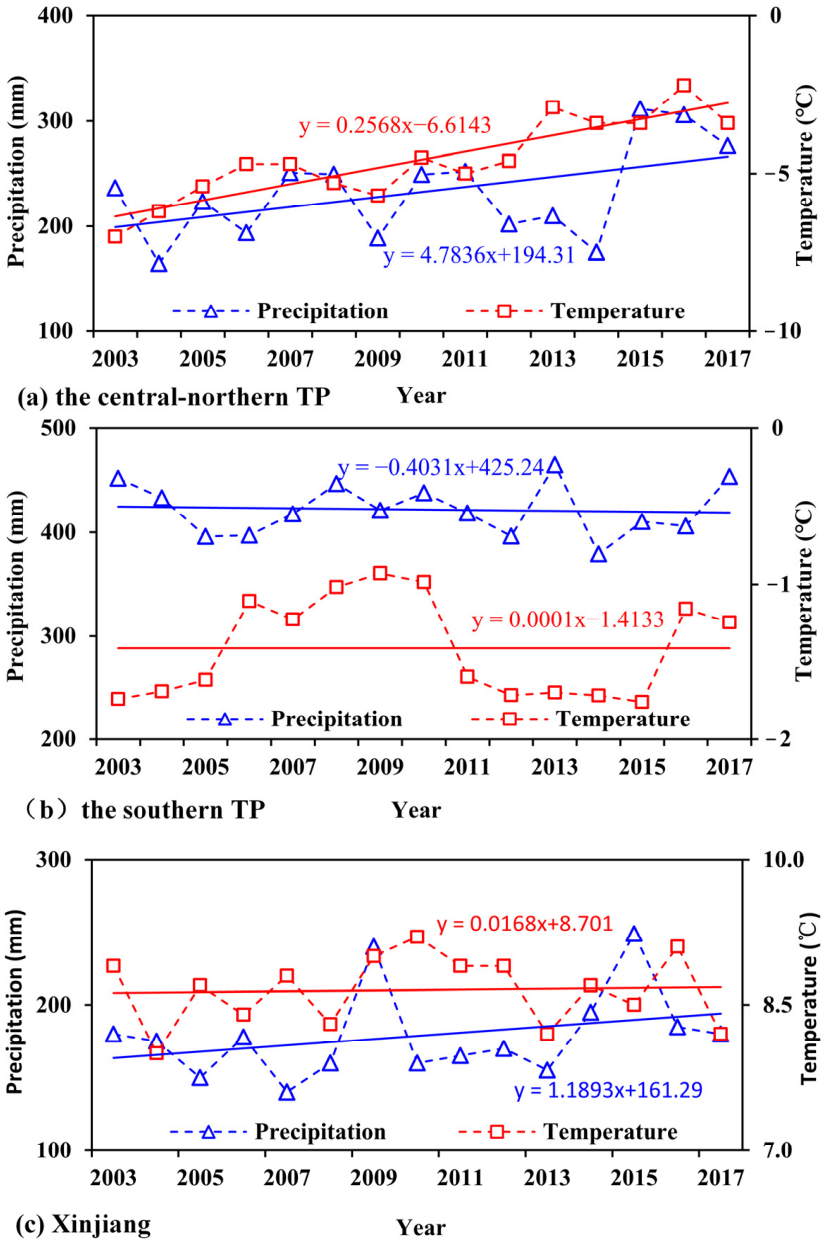

Figure 11. Annual variations in the mean precipitation and air temperature of the central–northern TP (**a**), the southern TP (**b**), and Xinjiang (**c**) from 2003 to 2017, derived from the TPDC grid data.

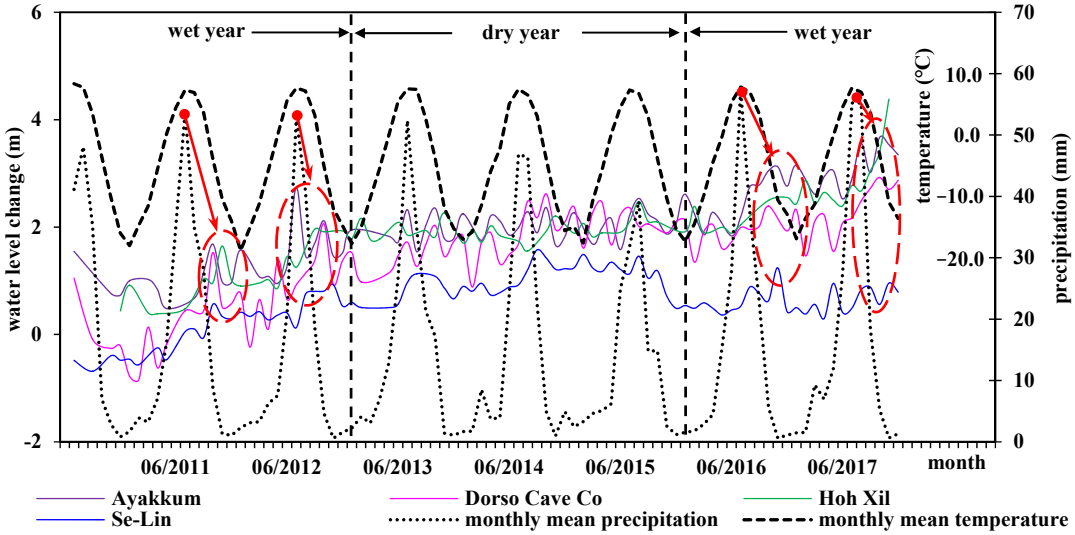

Figure 12. Comparison of the lake level monthly variations in four typical lakes, monthly mean precipitation, and air temperature over the Qiangtang endorheic region, derived from the CryoSat-2 and TPDC grid data. The red arrows and dashed ellipse exhibit the monthly precipitation peaks corresponding to the water levels rising sharply within a short period. It is worth noting that the wet years in this figure only indicate the years with abundant summer monsoon precipitation because summer precipitation can directly and significantly affect the lake levels.

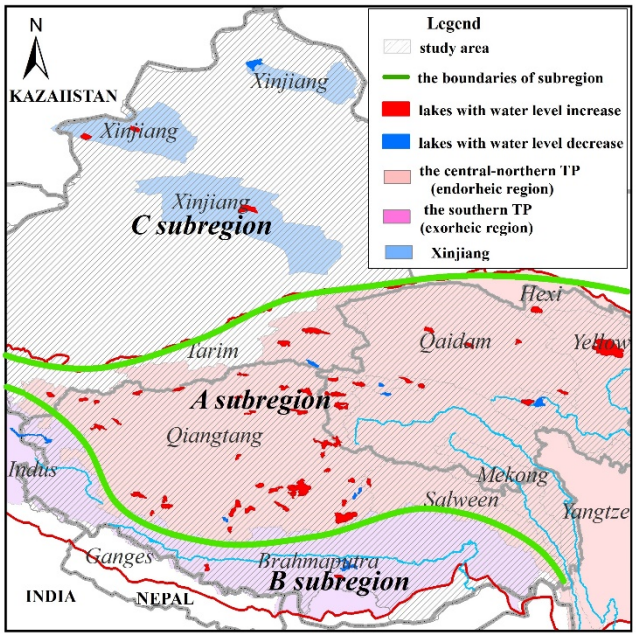

Figure 13. The classification of lake level changes in western China under different climate driving mechanisms. The plots are given in three different colors indicating the A, B, and C subregions. The lakes shown in red indicate the water level increased continuously and the lakes shown in blue indicate that the water level decreased continuously during 2003–2021.

6. Conclusions

This study combined data from the ICESat-1 laser altimeter and CryoSat-2 radar altimeter to monitor lake levels and their changes in a large number of 67 relatively small lakes in western China for the period 2003–2021. Our derived lake levels were validated with limited available in situ lake levels and good agreement was observed for Lake Nam Co. In addition, we compared the estimated trends of the lake level changes using our

derived lake levels and the well-validated DAHITI product, where good consistency was again found between them, indicating the good accuracy of our derived lake levels. A total of 51 of the studied 67 lakes had relatively complete ICESat-1 elevation data covering the period of 2003 to 2009, and almost all of the studied lakes had complete CryoSat-2 data from 2010 to 2021. Based on our derived lake levels, we found that 55 (82%) of these lakes showed a water level increasing tendency, and the remaining 12 (18%) of the lakes showed a water level decreasing tendency. Overall, the mean elevation change rate in western China is 0.15 m/yr (from −1.40 to 0.58 m/yr). The spatial patterns in the lake level variations can be grouped into three subregions: lake level changes between 2003 and 2021 showed general rising lake levels for the central–northern TP endorheic region and Xinjiang, but declining levels for the southern TP exorheic region. The seasonal characteristic of lake level changes showed a significant lake level increase during the summer monsoon season that was followed by decreases during the non-monsoon season. The precipitation variations played a leading role in the lake level changes in the context of warm and humid climate states, there was a good correspondence between the monthly variations of lake level and monthly mean precipitation. Additionally, the lake levels showed a relationship with air temperature change; in particular, the lake level increase showed a small degree of hysteresis behavior compared with the rising temperatures. Geographically, the precipitation increase in the westerlies regions has led to widespread lake expansion in the central–northern TP and Xinjiang (Region A and C). Conversely, a precipitation decrease in Indian monsoon regions has caused lake shrinkage in the exorheic region of the southern TP (Region B).

In the current warm and humid climate state, lakes in western China would continue to expand. In order to further understand the role of lake changes in the regional water cycle and climate change of the TP, it is necessary to fully understand the variation in the lake water storage and their continuous time series. This study used data from only ICESat-1 and CryoSat-2 satellite altimetry missions. While the results in this study demonstrate that satellite altimetry data are undoubtedly important for understanding the general features of seasonal lake level changes, more frequent observations are needed to depict the seasonality of lake hydrology and its spatial pattern. To achieve observations at higher temporal resolutions and for larger spatial coverage, it would be important to combine more satellite altimetry missions to cover more lakes and longer periods in future studies. In particular, the Surface Water and Ocean Topography (SWOT) mission to be launched in November 2022 will provide greater capability for the monitoring lake levels in more lakes than past and existing altimetry missions. More studies should also be focused on developing novel spatiotemporal densification methods to combine multiple satellite altimetry missions [58]. Furthermore, the remote sensing data, observations from high-density meteorological stations, together with advanced data assimilation and modeling techniques, are needed to further quantitatively clarify the mechanism of the lake changes in western China.

Author Contributions: J.C.: Conceptualization, methodology, data processing, and analysis, writing—original draft and review & editing. Z.D.: Conceptualization, methodology, writing—review & editing. All authors have read and agreed to the published version of the manuscript.

Funding: This work was supported by the National Natural Science Foundation of China (41901129). Zheng Duan acknowledges the support from the Joint China–Sweden Mobility Grant funded by NSFC and STINT (CH2019-8250).

Data Availability Statement: The DAHITI lake levels can be downloaded from https://dahiti.dgfi.tum.de/en/products/water-level-altimetry/ (accessed on 18 July 2022); The Cryosat-2 data can be downloaded at https://earth.esa.int/eogateway/missions/cryosat/data (accessed on 10 July 2022); ICESat-1 All GLA14 Release-33 laser altimetry data can be downloaded from the U.S. National Snow and Ice Data Center (NSID) at https://nsidc.org/data/ (accessed on 20 February 2022).

Conflicts of Interest: The authors declare no conflict of interest.

References

1. Lehner, B.; Doll, P. Development and validation of a global database of lakes, reservoirs and wetlands. *J. Hydrol.* **2004**, *296*, 1–22. [CrossRef]
2. William, Y.B.; Chang, W. Large Lakes of China. *J. Great Lakes Res.* **1987**, *13*, 235–249.
3. Qin, B.; Huang, Q. Evaluation of the Climatic Change Impacts on the Inland Lake—A Case Study of Lake Qinghai, China. *Resour. Res.* **1998**, *39*, 695–714.
4. Williams, W.D. Chinese and Mongolian saline lakes: A limnological overview. *Hydrobiologia* **1991**, *210*, 39–66. [CrossRef]
5. Revelle, R.R.; Waggoner, P.E. Effects of a Carbon Dioxide-Induced Climatic Change on Water Supplies in 7 the Western United States. *Chang. Clim.* **1983**, *496*, 419–432.
6. Guo, Z.; Miao, Q.; Li, X. Variation Characteristics of Temperature over Northern China in Recent 50 Years. *Entia Geogr. Sin.* **2005**, *25*, 448–454.
7. Liu, C.; Du, L.; Chen, X.; Qiao, X. The Change of Effectively Irrigated Land Area in China during the Past 20 Years. *Resour. Sci.* **2006**, *28*, 8–12.
8. Song, C.; Huang, B.; Ke, L.; Richards, K.S. Remote sensing of alpine lake water environment changes on the Tibetan Plateau and surroundings: A review. *Isprs. J. Photogramm.* **2014**, *92*, 26–37. [CrossRef]
9. Khanal, S.; Lutz, A.F.; Kraaijenbrink, P.D.A.; Hurk, B.V.D.; Immerzeel, W.W. Variable 21st Century Climate Change Response for Rivers in High Mountain Asia at Seasonal to Decadal Time Scales. *Water Resour. Res.* **2021**, *57*, e2020WR029266. [CrossRef]
10. Duan, Z.; Bastiaanssen, W. Estimating water volume variations in lakes and reservoirs from four operational satellite altimetry databases and satellite imagery data. *Remote Sens. Environ.* **2013**, *134*, 403–416. [CrossRef]
11. Peng, G. Remote sensing of environmental change over China: A review. *Sci. Bull.* **2012**, *57*, 2793–2801.
12. Chen, T.; Song, C.; Ke, L.; Wang, J.; Li, K.; Wu, Q. Estimating seasonal water budgets in global lakes by using multi-source remote sensing measurements. *J. Hydrol.* **2020**, *593*, 125781. [CrossRef]
13. Crétaux, J.F.; Jelinski, W.; Calmant, S.; Kouraev, A.; Vuglinski, V.; Bergé-Nguyen, M.; Gennero, C.M.; Nino, F.; Del Rio, R.A.; Cazenave, A.; et al. SOLS: A lake database to monitor in the Near Real Time water level and storage variations from remote sensing data. *Adv. Space Res.* **2011**, *47*, 1497–1507. [CrossRef]
14. Li, J.; Chen, X.; Bao, A. Spatial-temporal Characteristics of Lake Level Changes in Central Asia during 2003–2009. *Acta Geogr. Sin.* **2011**, *66*, 1219–1229.
15. Luo, R.; Yuan, Q.; Yue, L.; Shi, X. Monitoring Recent Lake Variations Under Climate Change Around the Altai Mountains Using Multimission Satellite Data. *IEEE J-STARS* **2020**, *14*, 1374–1388. [CrossRef]
16. Luo, S.; Song, C.; Zhan, P.; Liu, K. Refined estimation of lake water level and storage changes on the Tibetan Plateau from ICESat/ICESat-2. *Catena* **2021**, *200*, 105177. [CrossRef]
17. Zhang, G.; Xie, H.; Kang, C.; Yi, D.; Ackley, S. Monitoring lake level changes on the Tibetan Plateau using ICESat altimetry data (2003–2009). *Remote Sens. Environ.* **2011**, *115*, 1733–1742. [CrossRef]
18. Zhang, G.; Chen, W.; Xie, H. Tibetan Plateau's Lake Level and Volume Changes From NASA's ICESat/ICESat-2 and Landsat Missions. *Geophys. Res. Lett.* **2019**, *46*, 13107–13118. [CrossRef]
19. Jiang, L.; Nielsen, K.; Andersen, O.B.; Bauer-Gottwein, P. A bigger picture of how the Tibetan lakes change over the past decade revealed by CryoSat-2 altimetry. *J. Geophys. Res-Atmos.* **2020**, *125*, e2020JD033161. [CrossRef]
20. Kleinherenbrink, M.; Ditmar, P.G.; Lindenbergh, R.C. Retracking Cryosat data in the SARIn mode and robust lake level extraction. *Remote Sens. Environ.* **2014**, *152*, 38–50. [CrossRef]
21. Fan, C.; Song, C.; Li, W.; Liu, K.; Wang, J. What drives the rapid water-level recovery of the largest lake (Qinghai Lake) of China over the past half century? *J. Hydrol.* **2021**, *593*, 125921. [CrossRef]
22. Zhao, Y.; Liao, J.; Shen, G.; Zhang, X. Monitoring the water level changes in Qinghai Lake with satellite altimetry data. *J. Remote Sens.* **2017**, *21*, 633–644.
23. Zhang, G. *China Lake Dataset (1960s–2020)*; National Tibetan Plateau Data Center: Beijing, China, 2019.
24. Mcfeeters, S.K. The use of the Normalized Difference Water Index (NDWI) in the delineation of open water features. *Int. J. Remote Sens.* **1996**, *17*, 1425–1432. [CrossRef]
25. Kumari, N.; Srivastava, A.; Kumar, S. Hydrological Analysis Using Observed and Satellite-Based Estimates: Case Study of a Lake Catchment in Raipur, India. *J. Indian Soc. Remote Sens.* **2022**, *50*, 115–128. [CrossRef]
26. Labroue, S.; Boy, F.; Picot, N.; Urvoy, M.; Ablain, M. First quality assessment of the Cryosat-2 altimetric system over ocean. *Adv. Space Res.* **2012**, *50*, 1030–1045. [CrossRef]
27. Wingham, D.J.; Francis, C.R.; Baker, S.; Bouzinac, C.; Brockley, D.; Cullen, R.; de Chateau-Thierry, P.; Laxon, S.W.; Mallow, U.; Mavrocordatos, C. CryoSat: A mission to determine the fluctuations in Earth's land and marine ice fields. *Adv. Space Res.* **2006**, *37*, 841–871. [CrossRef]
28. Jain, M.; Jain, M.; Andersen, O.B.; Dall, J.; Stenseng, L. Sea surface height determination in the Arctic using Cryosat-2 SAR data from primary peak empirical retrackers. *Adv. Space Res.* **2015**, *55*, 40–50. [CrossRef]
29. Nielsen, K.; Stenseng, L.; Andersen, O.; Villadsen, H.; Knudsen, P. Validation of CryoSat-2 SAR mode based lake levels. *Remote Sens. Environ.* **2015**, *171*, 162–170. [CrossRef]

30. Chen, J.; Liao, J. Monitoring lake level changes in China using multi-altimeter data (2016–2019). *J. Hydrol.* **2020**, *590*, 125544. [CrossRef]
31. Guo, H.; Jiao, W.; Yang, Y. The Systematic Difference and Its Distribution between the 1985 National Height Datum and the Global Quasigeoid. *Acta Geod. Cartogr. Sin.* **2004**, *33*, 100–104.
32. Bhang, K.J.; Schwartz, F.W.; Braun, A. Verification of the Vertical Error in C-Band SRTM DEM Using ICESat and Landsat-7, Otter Tail County, MN. *IEEE Trans. Geosci. Remote Sens.* **2007**, *45*, 36–44. [CrossRef]
33. Zwally, H.J.; Yi, D.; Kwok, R.; Zhao, Y. ICESat measurements of sea ice freeboard and estimates of sea ice thickness in the Weddell Sea. *J. Geophys. Res. Ocean* **2008**, *113*, 1–17. [CrossRef]
34. Zwally, H.J.; Schutz, B.; Abdalati, W.; Abshire, J.; Bentley, C.; Brenner, A.; Bufton, J.; Dezio, J.; Hancock, D.; Harding, D.; et al. ICESat's laser measurements of polar ice, atmosphere, ocean, and land. *J. Geodyn.* **2002**, *34*, 405–445. [CrossRef]
35. Ding, M. *Temperature and Precipitation Grid Data of the Qinghai Tibet Plateau and Its Surrounding Areas in 1998–2017 Grid Data of Annual Temperature and Annual Precipitation on the Tibetan Plateau and Its Surrounding Areas during 1998–2017*; National Tibetan Plateau Data Center: Beijing, China, 2019.
36. Song, C.; Ye, Q.; Sheng, Y.; Gong, T. Combined ICESat and CryoSat-2 Altimetry for Accessing Water Level Dynamics of Tibetan Lakes over 2003–2014. *Water* **2015**, *7*, 4685–4700. [CrossRef]
37. Wang, J. *The lake Level Observation Data of Lake Namco from the Integrated Observation and Research Station of Multisphere in Namco (2007–2016)*; National Tibetan Plateau Data Center: Beijing, China, 2018.
38. Siddique-E-Akbor, A.; Hossain, F.; Lee, H.; Shum, C.K. Inter-comparison study of water level estimates derived from hydrodynamic–hydrologic model and satellite altimetry for a complex deltaic environment. *Remote Sens. Environ.* **2011**, *115*, 1522–1531. [CrossRef]
39. Schwatke, C.; Dettmering, D.; Bosch, W.; Seitz, F. DAHITI—An innovative approach for estimating water level time series over inland waters using multi-mission satellite altimetry. *Hydrol. Earth Syst. Sci.* **2015**, *19*, 4345–4364. [CrossRef]
40. Liu, Z.; Yao, Z.; Wang, R. Evaluation and Validation of CryoSat-2-Derived Water Levels Using In Situ Lake Data from China. *Remote Sens.* **2019**, *11*, 899. [CrossRef]
41. Busker, T.; Roo, A.D.; Gelati, E.; Schwatke, C.; Cottam, A. A global lake and reservoir volume analysis using a surface water dataset and satellite altimetry. *Hydrol. Earth Syst. Sci.* **2019**, *23*, 669–690. [CrossRef]
42. Li, X.; Long, D.; Huang, Q.; Han, P.; Zhao, F.; Wada, Y. High-temporal-resolution water level and storage change data sets for lakes on the Tibetan Plateau during 2000–2017 using multiple altimetric missions and Landsat-derived lake shoreline positions. *Earth Sysy. Sci. Data.* **2019**, *11*, 1603–1627. [CrossRef]
43. Xu, F.; Zhang, G.; Yi, S.; Chen, W. Seasonal trends and cycles of lake-level variations over the Tibetan Plateau using multi-sensor altimetry data. *J. Hydrol.* **2022**, *604*, 127251. [CrossRef]
44. Jiang, L.; Nielsen, K.; Andersen, O.B.; Bauer-Gottwein, P. Monitoring recent lake level variations on the Tibetan Plateau using CryoSat-2 SARIn mode data. *J. Hydrol.* **2017**, *544*, 109–124. [CrossRef]
45. Yang, R.; Yu, X.; Li, Y. The dynamic analysis of remote sensing information for monitoring the expansion of the selincuo lake in tibet. *Remote Sens. Land Resour.* **2003**, *2*, 64–67.
46. Li, L.; Wang, W. The response of lake change to climate fluctuation in north Qinghai-Tibet Plateau in last 30 years. *J. Geogr. Sci.* **2009**, *19*, 131–142.
47. Guo, Y.; Zhang, Y.; Ma, N.; Xu, J.; Zhang, T. Long-term changes in evaporation over Siling Co Lake on the Tibetan Plateau and its impact on recent rapid lake expansion. *Atmos. Res.* **2019**, *216*, 141–150. [CrossRef]
48. Zhu, L.; Zhang, G.; Yang, R.; Liu, C.; Yang, K.; Qiao, B.; Han, B. Lake Variations on Tibetan Plateau of Recent 40 Years and Future Changing Tendency. *Bull. Chin. Acad. Sci.* **2019**, *34*, 1254–1263. [CrossRef]
49. Yao, T.; Thompson, L.; Yang, W.; Yu, W.; Gao, Y.; Guo, X.; Yang, X.; Duan, K.; Zhao, H.; Xu, B.; et al. Different glacier status with atmospheric circulations in Tibetan Plateau and surroundings. *Nat. Clim. Change.* **2012**, *2*, 663–667. [CrossRef]
50. Lei, Y.; Yang, K.; Wang, B.; Sheng, Y.; Bird, B.W.; Zhang, G.; Tian, L. Response of inland lake dynamics over the Tibetan Plateau to climate. *Clim. Change* **2014**, *125*, 281–290. [CrossRef]
51. Qiao, B.; Zhu, L. Differences and cause analysis of changes in lakes of different supply types in the north-western Tibetan Plateau. *Hydrol. Process.* **2017**, *31*, 2752–2763. [CrossRef]
52. Lei, Y.; Yao, T.; Yang, K.; Sheng, R.; Kleinherenbrink, M.; Yi, S.; Bird, B.W.; Zhang, X.; Zhu, L.; Zhang, G. Lake seasonality across the Tibetan Plateau and their varying relationship with regional mass changes and local hydrology. *Geophys. Res. Lett.* **2017**, *44*, 892–900. [CrossRef]
53. Li, Y.; Liao, J.; Guo, H.; Liu, Z.; Shen, G. Patterns and Potential Drivers of Dramatic Changes in Tibetan Lakes, 1972–2010. *PLoS ONE* **2014**, *9*, e111890. [CrossRef]
54. Zhu, L.; Peng, P.; Zhang, G.; Qiao, B.; Wang, J. The role of Tibetan Plateau lakes in surface water cycle under global changes. *J. Lake Sci.* **2020**, *32*, 597–608.
55. Ye, Q.; Yao, T.; Zheng, H.; Zhang, X. Glacier and lake co-variations and their responses to climate change in the Mapam Yumco Basin on Tibet. *Geogr. Res.* **2008**, *27*, 1178–1190.

56. Lioubimtseva, E.; Henebry, C.M. Climate and environmental change in arid Central Asia: Impacts, vulnerability, and adaptations. *J. Arid. Environ.* **2009**, *73*, 963–977. [CrossRef]
57. Hu, R.; Yang, C.; Ma, H.; Jiang, F.; Urkunbek, A. Glaciers and lakes in the Tianshan mountains and climate trends. *Arid Land Geo.* **1994**, *17*, 1–9.
58. Tourian, M.J.; Tarpanelli, A.; Elmi, O.; Qin, T.; Brocca, L.; Moramarco, T.; Sneeuw, N. Spatiotemporal densification of river water level time series by multimission satellite altimetry. *Water Resour. Res.* **2016**, *52*, 1140–1159. [CrossRef]